arXiv:nucl-th/0204051v2 7 Jun 2005

In-Medium Effects in Eta Photo-production through the S_{11} Resonance with the Relativistic Approach

Tomoyuki Maruyama[1,2,3] and Satoshi Chiba[3]

[1] *College of Bioresource Sciences, Nihon University, Fujisawa, 252-8510, Japan*

[2] *Institute of Quantum Energy, Nihon University, Tokyo, 101-8308, Japan*

[3] *Advanced Science Research Center, Japan Atomic Energy Research Institute, Tokai 319-1195, Japan*

(Received January 28, 2003)

Abstract

In-medium effects in photon excitation of the S_{11} resonance from a nucleon and its decay into an η-meson are studied using the relativistic mean field approach. We examine the in-medium effects by varying the Dirac fields of the nucleon and the S_{11} resonance separately. We concluse that the Dirac fields of the nucleon, which reduce the nucleon effective mass, enlarge the width of the S_{11} resonance, and small Dirac fields of the resonance shift the peak position. These combined effects can account for the in-medium properties observed in the experimental data for ^{12}C(γ,η) reaction.

typeset using $\mathcal{PTP}$TEX.cls ⟨Ver.0.9⟩

§1. Introduction

Photon induced reactions are useful for obtaining information concerning the deep interior region of nuclei because photons are distorted little in the incident channel. Recent measurements of nuclear photo-absorption cross sections on several nuclei heavier than ^{7}Li$^{1)}$ have shown clear evidence of nuclear in-medium effects on isobar resonances: the resonance-like structures caused by the $D_{13}(1520)$ and $F_{15}(1680)$ excitations, clearly seen in the photo-absorption cross sections of hydrogen$^{2)}$ and deuteron,$^{3)}$ disappear in heavier nuclei, while the peak of the $P_{33}(1232)$ resonance still exists.

There have been several theoretical attempts to understand this disappearance.$^{4)-8)}$ At present, people are studiying the question of whether these phenomena are caused by the in-medium correction of the isobar resonances such as broadening of the width,$^{5)}$ or to other many-body processes such as interference in two-pion photo-production processes in the nuclear medium.$^{8)}$ Regarding the isobar width in medium, Kondratyuk et al.$^{6)}$ proposed that the collisional broadening plays a major role in the damping of the nucleon resonances in nuclei. However, Effenberger et al.$^{7)}$ showed that such a large increase of the resonance width is not supported justified by an estimation of the collision broadening based on the $N-N^*$ interaction.

In order to solve this problem, recently Yorita et al.$^{9),10)}$ carried out experiments on the $(\gamma,\ \eta)$ reaction with a carbon target to study the $S_{11}(1535)$ resonance. This resonance couples strongly with the $N\eta$ channel and has a large branching ratio for η decay. Because the elementary $H(\gamma,\eta)H$ reaction below 1.0 GeV can be described in terms of the excitation of the S_{11} resonance without any background process, it is reasonable to expect only the S_{11} resonance in (γ,η) reactions with nuclear targets. Furthermore, Yorita et al.$^{9),10)}$ analyzed their experimental data using the JAERI QMD code.$^{11)}$ From the comparison between their experimental data and the calculation results, they found an evidence that the width of the S_{11} resonance is broadened through the collisional process with nucleons.$^{9)}$ They were able to reproduce their data obtained using a C target with a resonance width of 212 MeV (+ collisional broadening) while the elementary $H(\gamma,\eta)H$ cross section is described better with a width of 154 MeV.$^{12)}$

This QMD calculation includes effects of the final state interaction, such as the absorption and multi-step collisions, and collisional broadening. In this analysis the peak shift is the most clear evidence showing the discrepancy between the theoretical calculation and the experimental data. The peak position of the incident photon energy for the cross section obtained theoretically is about 80 MeV lower than that observed experimentally if only the Fermi motion of the nucleon is considered in the calculation. The final state interaction from the absorption and the multi-step collisional processes shifts the peak in the direction of higher energy by about 20 MeV to higher energy, and the collisional broadening causes further shift of about 20 MeV. Thus, the final peak-position is lower than the observed one by approximately 40 MeV. Therefore we need to consider other in-medium effects to account for the experimental results.

Bolkland and Sherif$^{13)}$ and Peters et al.$^{14)}$ have calculated the exclusive photo-production of η meson with the DWIA using the relativistic mean field (RMF) approach.$^{15)}$ However, because there are no exclusive data, unfortunately, they could not compare their results with the experimental data and hence did not reach any meaningful conclusion. However, their works provide a hint to understand the problem discussed above from the perspective of relativistic theory. In the RMF approach, there are two kinds of Dirac mean fields, namely, large attractive scalar and repulsive vector fields, which lead to a small effective mass of the nucleon in the medium. The variation of the Dirac mean fields changes the excitation energy and the width of the isobar resonance because they depend on the effective mass of the nucleon, like the isobar resonance itself.

In this paper we investigate the in-medium effects in the S_{11} resonance excitation from nucleon and its decay into an η-meson by introducing the mean fields of the resonance within the RMF approach. Then, we can examine the in-medium effects by varying the Dirac fields of the nucleon and the S_{11} resonance separately. As the first step, actual calculations are performed for nuclear matter, and we focus our investigation on the peak position of the cross section rather than the absolute values.

In the next section we give the formulation of our model. Because the interaction between isobars and nucleons is not completely clear, we cannot carry out a complete microscopic calculation. For this reason, we propose a model that is partially microscopic and partially phenomenological. In Sec. 3 we give some results, and we summarize our study in Sec.4.

§2. Formalism

In this section we briefly explain our formalism. Unfortunately, isobar resonances have not yet been scuccessfully described with the standard field theoretical scheme. Their selfenergies and propagators cannot be consistently obtained from certain Lagrangians in the relativistic framework. All expressions have to be constructed phenomenologically.

On the other hand, phenomenological studies based on the Breit-Wigner formula$^{16)}$ have succeeded in explaining various experimental results with regard to the meson production and absorption. The Breit-Wigner formula is constructed under simple assumptions, and it can be easily derived in the nonrelativistic framework, but it is independent of the details of the interaction. To analyze the experimental results, hence, we must construct a theoretical model that is consistent with the Breit-Wigner formula. Our approach explained in this section is formulated according to this requirement.

First, we define the coupling of the S_{11} resonance, the nucleon and the photon in our model. We calculate the photo-absorption cross section with the impulse approximation, so that the calculational results are gauge-independent. Using the Coulomb gauge, then, we use the simplest form of the interaction Lagrangian between nucleon, the S_{11} resonancne and the photon as,

$$\mathcal{L}_{\mathrm{elmag}} = \tilde{g}_e \bar{\psi}_R \gamma_5 \vec{\gamma} \psi_N \vec{A} + \mathrm{h.c.}\ , \tag{2·1}$$

where ψ_N, ψ_R and A^μ are the nucleon, S_{11} resonance, and photon fields, respectively. In addition, $\tilde{g}_e$ is a coupling constant, which is determined from the experimental data. As is well known, the final results are frame independent under the Lorentz transformation, if we consider only photo-absorption or photo-emission. As discussed later, we choose the above interaction, which is different from that in Ref. 13), 14), in order for our treatment to be consistent with conventional treatments of the elementary process.

Now we study eta production in photo-absorption with the impulse approximation in terms of the RMF approach. We define the initial photon momentum q as

$$q = (Q; \boldsymbol{q}) = (Q; 0, 0, Q). \tag{2·2}$$

The photo-absorption cross section is proportional to the transverse response function:

$$\sigma_{abs} \propto \frac{1}{Q} \mathit{\Pi}_T. \tag{2·3}$$

The transverse response function $\mathit{\Pi}_T$ is defined as the imaginary part of the transverse polarization function:

$$\mathit{\Pi}_T(q) = \mathrm{Im}\{C_{11}(q) + C_{22}(q)\}. \tag{2·4}$$

Hence, the polarization function for the excitation between nucleon and the resonance is defined as

$$C_{ij}(q) = -i \int \frac{d^4p}{(2\pi)^4} \mathrm{Tr}\{S_R(p+q)\gamma_5\gamma_i S_N(p)\gamma_5\gamma_j\}\ , \tag{2·5}$$

where, S_N and S_R are the nucleon and S_{11} resonance propagators, respectively.

The nucleon propagator S_N involves the vacuum part and the density-dependent part, which describe nucleons occupying states below the Fermi energy of the system:

$$S_N(p) = (p^*_\mu \gamma^\mu + M^*_N) \left\{ \frac{1}{p^{*2} - M^{*2}_N + i\delta} + \frac{i\pi}{E^*_N(\boldsymbol{p})} n(\boldsymbol{p}) \delta(p_0 - \varepsilon_N(\boldsymbol{p})) \right\}, \tag{2·6}$$

where $n(\boldsymbol{p})$ is given by $n(\boldsymbol{p}) = \theta(p_F - |\boldsymbol{p}|)$ with the Fermi momentum p_F. In this expression, M^* and p^*_μ are the effective mass and the kinetic momentum, defined as

$$M^*_N = M_N - U_s(N), \tag{2·7}$$

$$p^*_\mu = p_\mu - U_\mu(N), \tag{2·8}$$

where U_s and $U_\mu = U_0\delta^0_\mu$ are the scalar and vector mean fields. In addition, the effective kinetic energy $E^*_N(\boldsymbol{p})$ and the single particle energy $\varepsilon_N(\boldsymbol{p})$ are defined as

$$E^*_N(\boldsymbol{p}) = \sqrt{\boldsymbol{p}^2 + M^{*2}_N}, \tag{2·9}$$

$$\varepsilon_N(\boldsymbol{p}) = E^*_N(\boldsymbol{p}) + U_0. \tag{2·10}$$

Similarly, we take the propagator of the S_{11} resonance with scalar and vector fields $U_s(R)$ and $U_\mu(R) = U_0(R)\delta^0_\mu$ to be

$$S_R(p) = \frac{p^*_{R\mu}\gamma^\mu + M^*_R}{p^{*2}_R - M^{*2}_R - i\sqrt{p^{*2}_R}\,\varGamma_R} \tag{2·11}$$

with

$$M^*_R = M_R - U_s(R), \tag{2·12}$$

$$p^*_{R\mu} = p_\mu - U_\mu(R). \tag{2·13}$$

The denominator of Eq. (2·11) is derived using the Breit-Wigner ansatz.7), 14), 16)

Because the nucleon and meson that decay from the S_{11} resonance are coupled in the s-wave, the energy dependence of the width of S_{11} is determined by the phase-space volume of decayed particles and the form factor of the resonance. Its expression is given in Ref. 16) as

$$\varGamma_R = \varGamma_\pi + \varGamma_\eta = \varGamma_0\left[b_\pi\frac{k(\pi)}{k_0(\pi)}x_\pi + b_\eta\frac{k(\eta)}{k_0(\eta)}x_\eta\right] \tag{2·14}$$

where $k(\pi)$ and $k(\eta)$ are momenta of the decayed pion and eta in the rest frame of the resonance, $k_0(\pi)$ and $k_0(\eta)$ are the pion and eta momenta at the resonance pole ($s_R = M^2_R$), b_π and b_η are the branching parameters for pion and eta channels, and x_π and x_η are the form factors given by

$$x_\pi = \frac{k^2_0(\pi) + c^2_\pi}{k^2(\pi) + c^2_\pi} \quad , \qquad x_\eta = \frac{k^2_0(\eta) + c^2_\eta}{k^2(\eta) + c^2_\eta}, \tag{2·15}$$

where c^2_π and c^2_η are determined from experimental data.17)

The width must be modified by the Pauli-blocking effect of decayed nucleons as well as by the mean fields. To include this effect, we define the width of the resonance in the medium as a function of the phase space. When the nucleon with momentum p absorbs the photon and is excited to the resonance, the phase space volume of the decayed particle becomes

$$k^2(i) \to \langle k_i^2 \rangle = \frac{1}{4\pi} \int d^3k \delta(k - k_N) \tag{2·16}$$

where

$$k_N^2 = \frac{1}{4s_{\text{eff}}} \{(s_{\text{eff}} - M_N^{*2} - m_i^2)^2 - 4s_{\text{eff}} M_N^{*2}\} \tag{2·17}$$

with

$$s_{\text{eff}} = (p^* + q)^2. \tag{2·18}$$

We transform the above integration in the rest frame of the resonance into the laboratory frame and add the Pauli-Blocking factor $(1 - n(\boldsymbol{p}'))$. Then we obtain

$$< k_i^2 >= \frac{\sqrt{s_{\text{eff}}}}{2|\boldsymbol{p}_R|} k_N \int_{p_-}^{p_+} dp' \frac{p'}{E_N^*(\boldsymbol{p}')} (1 - n(\boldsymbol{p}')) \tag{2·19}$$

with

$$\boldsymbol{p}_R = \boldsymbol{p} + \boldsymbol{q} \tag{2·20}$$

$$p_\pm = \frac{1}{\sqrt{s_{\text{eff}}}} |\{E_N^*(\boldsymbol{p})|\boldsymbol{p}_R| \pm (E_N^*(\boldsymbol{p}) + Q)k_N\}|. \tag{2·21}$$

Within the impulse approximation, only contribution to the response function (2·4) comes from the density-dependent part for the nucleon propagator (2·6) and the imaginary part of the resonance propagator (2·11):

$$S_N(p) \approx \frac{i\pi}{E_N^*(\boldsymbol{p})} n(\boldsymbol{p})(p_\mu^* \gamma^\mu + M_N^*)\delta(p_0 - \varepsilon_N(\boldsymbol{p})). \tag{2·22}$$

$$S_R(p) \approx -i(p_{R\mu}^* \gamma^\mu + M_R^*) \frac{\sqrt{p_R^{*2}} \mathit{\Gamma}_R}{(s_R^* - M_R^{*2})^2 + p_R^{*2} \mathit{\Gamma}_R^2}. \tag{2·23}$$

Substituting these equations into Eq.(2·5), we obtain the transverse response function $\mathit{\Pi}_T$. When this is done, we must multiply S_R by $\mathit{\Gamma}_\eta / \mathit{\Gamma}_R$ in Eq.(2·5) before integrating over the Fermi distribution in order to account only for the eta decay of the resonance.

As shown in Eq.(2·3), $\mathit{\Pi}_T / Q\rho_B$ is proportional to the contribution to the cross section from one nucleon. Therefore, we define the arbitrary normalization factor $\mathcal{A}_p$ for a proton and $\mathcal{A}_n$ for a neutron and obtain the eta photo-production cross section of the nuclear target with proton number Z and neutron number N

$$\sigma_\eta = (\mathcal{A}_p Z + \mathcal{A}_n N) \frac{4\mathcal{F}_{abs}}{\rho_B Q} \int \frac{d^3\boldsymbol{p}}{(2\pi)^3} n(\boldsymbol{p}) W_T \sqrt{s_R^*} f(s_R^*) \frac{\mathit{\Gamma}_\eta(s_{\text{eff}})}{\mathit{\Gamma}_R(s_{\text{eff}})}. \tag{2·24}$$

Here,

$$s_R^* = (p + q^*)^2, \tag{2·25}$$

where q^* is effective photon momentum defined as

$$q^* = (Q_0^*; 0, 0, Q) = (Q + U_0(N) - U_0(R); 0, 0, Q), \tag{2·26}$$

and W_T is defined as

$$W_T = W_{11} + W_{22}, \tag{2·27}$$

with

$$W_{\mu\nu} = \frac{1}{4E_N^*(\boldsymbol{p})\sqrt{s_R^*}} \mathrm{Tr}\{\gamma_\mu \gamma_5 (\not{p}^* + \not{q}^* + M_R^*)\gamma_5 \gamma_\nu (\not{p}^* + M_N^*)\}. \tag{2·28}$$

Here, the detailed expression of W_T in Eq. (2·24) becomes

$$W_T = \frac{2}{E_N^*(\boldsymbol{p})\sqrt{s_R^*}} \{E_N^{*2}(\boldsymbol{p}) - p_z^2 + E_N^*(\boldsymbol{p})Q_0^* - p_z Q + M_N^* M_R^*\}. \tag{2·29}$$

In addition, the function $f(s_R^*)$ in Eq.(2·24) is given with

$$f(s_R^*) = \frac{\sqrt{s_R^*}\mathit{\Gamma}_R}{(s_R^* - M_R^{*2})^2 + s_R^* \mathit{\Gamma}_R^2}, \tag{2·30}$$

where $\mathit{\Gamma}_\eta / \mathit{\Gamma}_R$ represents the decay ratio of the eta from the resonance, and $\mathcal{F}_{abs}$ is the absorption factor for eta propagation, which is taken to be arbitrary in this work.

We determine the normalization factor $\mathcal{A}_p$ from the elementary cross section of the $\gamma + p \to \eta$ reaction. In our model, this cross section is obtained from Eq.(2·24) as

$$\sigma_1^{el} = 2\mathcal{A}_p \frac{M_N + M_R + Q}{Q} f(s_R) \frac{\mathit{\Gamma}_\eta}{\mathit{\Gamma}_R}, \tag{2·31}$$

where $s_R = (p + q)^2$ with $p = (M_N; 0, 0, 0)$. On the other hand, this cross section is usually parametrized in the Breit-Wigner form$^{7),17)}$ as

$$\sigma_\eta^{BW} = |A_{\frac{1}{2}}(p)|^2 \frac{M_N(M_R^2 - M_N^2)}{M_R^2 Q_c} \sqrt{s_R} f(s_R) \frac{\mathit{\Gamma}_\eta}{\mathit{\Gamma}_R}, \tag{2·32}$$

where Q_C is the photon momentum in the center-of-mass system of the incident photon and proton. We can rewrite this in the laboratory frame as

$$\sigma_\eta^{BW} = |A_{\frac{1}{2}}(p)|^2 \frac{M_R^2 - M_N^2}{M_R^2 Q} s_R f(s_R) \frac{\mathit{\Gamma}_\eta}{\mathit{\Gamma}_R}, \tag{2·33}$$

using

$$Q_C = \frac{Q M_N}{\sqrt{s_R}}. \tag{2·34}$$

From the condition that $\sigma_1^{el} = \sigma_\eta^{BW}$ at $s_R = M_R^2$ we can determine the factor $\mathcal{A}_p$ to be

$$\mathcal{A}_p = \frac{M_N(M_R - M_N)}{(M_R + M_N)} |A_{\frac{1}{2}}(p)|^2 \tag{2·35}$$

Furthermore, the relation between $\mathcal{A}_p$ and $\mathcal{A}_n$ is given in Refs. 7), 17) as

$$\mathcal{A}_n = \frac{2}{3}\mathcal{A}_p. \tag{2·36}$$

Here we give a comment. W_T exhibits a relativistic effect through the Lorentz transformation property of the Dirac spinor, and therefore W_T becomes constant in the nonrelativistic limit. Such a nonrelativistic scheme actually gives the Breit-Wigner form$^{7),17)}$ for the cross section of the eta photo-production for the proton target. In the center-of-mass system, in fact, the cross section σ_η^{BW} is equivalent to our expression when W_T is taken to be $W_T = W_T^{NR}(CM)$ given as

$$W_T^{NR}(CM) = \frac{(M_R + M_N)^2}{M_R^2}. \tag{2·37}$$

In the laboratory frame, in addition, this W_T becomes

$$W_T^{NR}(L) = \frac{(M_R + M_N)^2 \sqrt{s_R}}{M_R^2 M_N} = \frac{(M_R + M_N)^2}{M_R^2} \sqrt{\frac{(M_N + 2Q)}{M_N}}. \tag{2·38}$$

Here, we should give one more comment. In Refs.13),14) a Lagrangian that differs from ours is used. It is given by

$$\mathcal{L}^{(2)}_{\text{elmag}} = \tilde{\kappa}_e \bar{\psi}_R \gamma_5 \sigma_{\mu\nu} \psi_N F^{\mu\nu} + \text{h.c. }. \tag{2·39}$$

Using this Lagrangian density, the $p(\gamma,\eta)$ cross section is obtained in the same way as

$$\sigma_2^{el} = \frac{4M_N^2 Q}{M_R(M_R^2 - M_N^2)} |A_{\frac{1}{2}}(p)|^2 f(s_R) \frac{\Gamma_\eta}{\Gamma_R}. \tag{2·40}$$

The above cross section σ_2^{el} differs from σ_1^{el} and σ_{BW}^{el} by a factor of Q^2 in the limit $Q \to 0$, because W_T is proportional to Q^2 in this limit. Thus, this electromagnetic interaction is inconsistent with the Breit-Wigner formula, and therefore it cannot be used for the analysis of experimental data.

Contrastingly, the Lagrangian we chose has the simplest form that satisfies the s-wave coupling in the low-energy limit. Our expression can indeed reproduce the phenomenological cross section and the experimental data for the elementary process as shown in Fig.1. This implies that the Lagrangian we have chosen is reasonable for our purpose. Recently a similar electromagnetic interaction was derived using a vector dominat model in Ref. 18). Our method must corresponds to an approximation of this vector dominant approach.

The numerical difference between σ_1^{el} and σ_2^{el} is presented in the next section.

§3. Results and Discussion

In this section we reports the results of actual calculations. The parameter values for the S_{11} resonance are taken as $M_R = 1.540$ GeV, $\Gamma_0 = 0.15$ GeV, $b_\eta = 0.55$, and $c_\pi^2 = c_\eta^2 = 0.25$ GeV^2.

In Fig. 1 we plot our result (σ_1^{el}) with a solid curve, and the experimental data$^{12),17)}$ are indicated by the filled circles and squares. Our result reproduces the experimental data quite well. Furthermore, we plot the cross section σ_2^{el} (2·40) obtained with the Lagrangian density $\mathcal{L}^{(2)}$ in Eq.(2·39) with the dashed curve, while the best-fit phenomenological expression σ_η^{BW} is represented by the dotted curve. We can see that σ_2^{el} does not agree with either σ_1^{el} or σ_η^{BW}, at least when the same values of the resonance mass M_R and width $\mathit{\Gamma}_0$ are used.

As commented above, the difference between σ_1^{el} and σ_η^{BW} lies in W_T defined in Eq. (2·27), which is obtained from the Lorentz transformation property of the Dirac spinor. The agreement of two results implies that the relativistic effects, except for the kinematics, are not important in this elementary reaction.

Next, we examine in-medium effects through the Dirac fields. The parameter-sets for the nuclear selfenergies are taken from PM1[19)] (namely, $BE = 16$ MeV, $M^*/M = 0.7$ at $\rho_0 = 0.17\text{fm}^{-3}$). By contrast, we do not have any information on the S_{11} resonance mean fields. However, it is not unnatural to assume that the S_{11} resonance potential is not large:

$$\frac{|U_s(R) - U_0(R)|}{M_R} \ll 1 \tag{3·1}$$

Then, we fix the ratio of the nucleon and the S_{11} resonance self-energies as

$$u_r = \frac{U_s(R)}{U_s(N)} = \frac{U_0(R)}{U_0(N)}, \tag{3·2}$$

and examine the effects of the S_{11} resonance mean fields by varying the ratio u_r. Of course, $U_s(R)$ and $U_0(R)$ can be varied independently, but this variation is restricted to only a few tens of MeV by the condition (3·1), while the depth of the mean fields is about several hundred MeV. Such small variation is not thought to affect the results of qualitative studies.

In the actual calculation we omit the Pauli blocking factor in Eq. (2·19), because the photon momentum is very large, and this factor does not contribute to the results of the calculation. In addition, the value of the normalization constant $\mathcal{F}_{abs}$ was determined to reproduce the experimental data at the peak. Here, we take $\mathcal{F}_{abs} = 0.83$. This value is not very far from the value obtained from the QMD approach ($\mathcal{F}_{abs} = 0.75$ around $Q = 850$MeV).[9)]

In Fig. 2, we compare the results for the photo-production of η with the experimental data in the case of ^{12}C target. The solid curve, long-dashed curve and dashed curve represent the results for $u_r = 0$, $u_r = 0.5$ and $u_r = 1$, respectively. We can see that the result agrees well with the experimental data in the case $u_r = 0$.

Now we give qualitative discussions of the peak photon energy. The peak energy for the mass distribution function (2·30) is given by $s_R^* = M_R^{*2}$. When integrating over Fermi sea, the actual peak energy is close to the energy corresponding to the condition that the absorbed photon excites a rest nucleon to the resonance with mass M_R^*, that is,

$$M_R^{*2} = (M_N^* + U_0(N) - Q)^2 - Q^2 \tag{3·3}$$

We define $\bar{Q}$ form the above condition as

$$\bar{Q} = \frac{M_R^{*2} - (M_N + U_c(N))^2}{2(M_N + U_c(N))} \tag{3·4}$$

with

$$U_c(N) = -U_s(N) + U_0(N). \tag{3·5}$$

When $U_{s,0}(R) = 0$, which corresponds to the case $u_r = 0$, we have

$$\begin{aligned} \bar{Q} &= \frac{M_R^2 - (M_N + U_c(N))^2}{2(M_N + U_c(N))} \\ &\approx \frac{M_R^2 - M_N^2}{2M_N} - \frac{M_R^2 + M_N^2}{2M_N^2} U_c(N). \end{aligned} \tag{3·6}$$

This $U_c(N)$ is almost identical to the central potential of a nucleon in the nonrelativistic picture. This value of $\bar{Q}$ is slightly larger than the real peak energy, because of the factor $1/Q$ appearing in the equation. Substituting the values of the mean fields into the above Eq. (3·6), we obtain that $\Delta\bar{Q} = \bar{Q} - \bar{Q}_0 = 120$ MeV, while the actual peak shift is about 80 MeV. This analysis thus overestimates the peak shift. When $M_N^* = M_N$ $[U_s(N) = 0]$ with the fixed Fermi energy, in addition, the vector field $U_0(N) = -54$ (MeV), and we obtain $\Delta\bar{Q} = \bar{Q} - \bar{Q}_0 = 100$ MeV. We thus conclude that the binding effect of nucleons partially accounts for the peak shift, but it is not perfect.

In Fig. 3 we display the results for $u_r = 0$ with $M_N^*/M_N = 0.7$ (solid curve) and $M_N^*/M_N = 1$ (dotted-dashed curve). The peak shift at $M_N^*/M_N = 1$ is about 40 MeV, while that at $M_N^*/M_N = 0.7$ is about 80 MeV. In the case $M_N^*/M_N = 1$, in addition, the width is smaller than that at $M_N^*/M_N = 0.7$. This result indicates that the in-medium correction of the nucleon mass also contributes to the broadening of the width.

To confirm the above claim, we consider the momentum-dependent width of the S_{11} resonance in medium. In Fig. 4, we display the width of the resonance, which is created from the rest nucleon, $\Gamma_{\rm r}(\eta) = \Gamma_\eta/(b_\eta \Gamma_0)$. The results are plotted as functions of the incident photon energy for $u_r = 0$ with $M_N^*/M_N = 0.7$ (solid curve) and $M_N^*/M_N = 1$ (dotted-dashed curve) in Fig. 4(a), and the same results are also plotted as functions of $\sqrt{s_{\rm eff}}$ in Fig. 4(b).

The small effective mass of the nucleon increases the phase space of the decayed particle and enlarges the width for small value of the effective invariant mass $s_{\rm eff}$ (see Fig.4(b)). For the rest nucleon, however, the effective invariant mass becomes

$$s_{\rm eff} = M_N^*(M_N^* + 2Q). \tag{3·7}$$

Thus the small effective mass also reduces the effective invariant mass at the fixed energy of the incident photon. Therefore the width with a small nucleon effective mass is smaller in the low photon momentum region and larger in the high momentum region. This effect also shifts the peak and broadens the actual width of the mass distribution function of the resonance in the medium.

The fact that $u_r = 0$ is preferred, is similar to the finding of Yorita's analysis given in Ref. 9) that a small binding effect and the enhanced width of the resonance in medium can yield results that reproduce the experimental data.

Finally, we examine relativistic effects other than the kinematics by changing the method to relate the elementary cross section with the in-medium one. As mentioned before, W_T exhibits a relativistic effect through the Lorentz transformation property of the Dirac spinor, and W_T becomes constant in the nonrelativistic limit. Therefore we substitute $W_T^{NR}(L)$ of Eq. (2·38) into Eq. (2·24) and integrate the latter over nucleon momenta below Fermi level. This calculation corresponds to folding the phenomenological elementary cross section σ_η^{BW}. We refer to the results obtained with this cross section as C2, while the results given above (σ^{eta}) are referred to as C1.

Furthermore, we consider the situation in which the rest nucleon in the nuclear medium absorbs the photon with momentum $Q = \bar{Q}$. In this case, W_T becomes $W_T^{\rm eff}$ defined as

$$W_T^{\rm eff} = \frac{(M_R^* + M_N^*)^2 \sqrt{s_{\rm eff}}}{2M_R^{*2} M_N^*}. \tag{3·8}$$

Then, we refer to the results of the calculation employing W_T^{eff} instead of W_T as C3.

In Fig. 5 the results are displayed. There the solid, dashed and dotted curves represent the results calculated C1, C2 and C3, respectively. The calculations were carried out using at $M_N^*/M_N = 0.7$ and with $u_r = 0$ (Fig 5(a)) and with $u_r = 1$ (Fig 5(b)). While the three sets of the results are almost the same for $u_r = 0$ (Fig 5(a)), C3 is slightly smaller than others (Fig. 5(a)). Contrastingly, three results are almost the same for $u_r = 1$ (Fig. 5(b)). As commented above, this difference comes from W_T defined in Eq. (2·27), which is obtained from the Lorentz transformation property of the Dirac spinor. This relativistic effect is, however, not so large; only a small effective mass contributes to the results.

As stated previously, the purpose of this paper is to qualitatively study the peak shift and broadening width in view of the kinematics, and we are not presently concerned with analyzing the absolute value of the cross section. The results obtained with the three kinds of calculations (C1, C2 and C3) have nearly same shapes, and their peak positions coincide. Only the peak of C2 with $u_r = 0$ is shifted to a position higher than that of the others by about 20 MeV, but this difference is not very significant. In this respect, our calculation using Lagrangian Eq.(1) can be verified.

§4. Summary

In this paper we investigated in-medium effects for eta photo-production. We used the RMF approach and calculated the eta production cross section, varying the Dirac fields of the S_{11} resonance. We find that small Dirac fields of the S_{11} resonance gives the best results, though the nucleon fields are not small. This result can be explained with the following mechanism.

The small Dirac-fields of the S_{11} resonance shift the peak to higher energy through binding effects, and the small effective mass of the nucleon enlarges the width. The deep resonance Dirac-fields also enlarge the width, but they suppress the peak shift, and they cannot account for the experimental data. In other words the difference between the mean fields of the nucleon and the resonance modifies the kinematical relation in-medium between them and changes the shape of the eta photo-production cross section.

When extending the elementary cross section to the in-medium case, there is a difference between our results and those obtained using the phenomenological elementary cross section that corresponds to the nonrelativistic one. This difference is caused by the small effective mass in the nuclear medium. In any case, this effect only changes the absolute value and does not change our discussion on the peak and width of the cross section.

Of course, there are several ambiguities in our treatment, and for this reasons, we cannot give a perfectly quantitative conclusion at present. Regardng the photo-absorption process, we must take account of the collisional broadening of the resonance width in the future. In addition, the final state interaction also contributes to the peak shift; the eta absorption from the nucleon is energy-dependent, and hence the absorption factor must also be energy dependent. It is confirmed in Ref. 9) that this energy-dependence of the absorption and the multi-step process shift the peak position toward higher energy, though this final state interaction, together with the collisional broadening, is not sufficient to accout for the experimental data. The effects we elucidated in this paper are supposed to be smaller in finite nuclei, and the collisional broadening and the final state interaction must contribute to the peak shift. It is expected that the cooperating effects of the Dirac-fields and the final state interaction account for the peak shift and the width of the cross section. Thus, we need to calculate the cross section for finite nuclei including realistic eta absorption and multi-step effects. For this purpose, the RBUU approach should be useful.23),24) In such a work, we may consider in-medium corrections for eta absorption and collisions between S_{11} and nucleon. In addition, we may take account of coherent effects for eta production.14),25)

It has recently beenn suggestted that the S_{11} resonance is the chiral partner of the nucleon.26)

The development of this study may suggest other restrictions that can eliminate for the ambiguities. Furthermore, the in-medium modification of η properties has been suggested from this chiral partner model.$^{27)}$ These effects may change the peak energy and width of the cross section. We should take into account such in-medium corrections in the future.

We would like to give several further comments. From this work, we learn that the peak position and the width of the cross section are determined by in-medium modification of the kinematical relation between the isobar resonance and decayed particles. We conclude that the $S_{11}(1535)$ resonance does not have large in-medium effects. On the other hand, we need to introduce more drastic effects to account for the experimental data for $\mathrm{D}_{13}(1520)$ and $\mathrm{F}_{15}(1680)$. There is a strong possibility that the in-medium correction of the ρ-meson is one effect that can be useful in this regard.

Acknowledgments

We would like thank Prof. J. Kasagi and Dr. H. Yamazaki for useful discussion and providing us with experimental data.

References

1) Th. Frommhold *et al.*, Phys. Lett. B295 (1992), 28; M. Anghinolfi *et al.*, Phys. Rev. C47 (1993), R922; N. Bianchi *et al.*, Phys. Lett. B299 (1993), 219, Phys. Lett. B309, (1993) 5, Phys. Rev. C54 (1996), 1688.
2) T. A. Armstrong *et al.*, Phys. Rev. D5 (1972), 1640.
3) T. A. Armstrong *et al.*, Nucl. Phys. B41 (1972), 445.
4) M. M. Giannini and E. Santopinto, Phys. Rev. C49 (1994), R1258.
5) W. M. Alberico, G. Gervino and A. Lavagno, Phys. Lett. B321 (1994), 177.
6) L. A. Kondratyuk *et al.*, Nucl. Phys. A579 (1994), 453.
7) M. Effenberger, A. Hombach, S. Teis and U. Mosel, Nucl. Phys. A613 (1997), 353; Nucl. Phys. A614 (1997), 501.
8) M. Hirata, K. Ochi and T. Takaki, Phys. Rev. Lett.80 (1998), 5068.
9) T. Yorita et al, Phys. Lett. B476 (2000), 226.
10) T. Yorita, PhD-thesis.
11) K. Niita, S. Chiba, T. Maruyama, T. Maruyama, H. Takada, T. Fukahori, Y. Nakahara and A. Iwamoto, Phys. Rev. C52 (1995), 2620;
T. Maruyama and A. Iwamoto, Phys. Rev. C53 (1996), 1824.
12) F. Renard et al., hep-ex/0011098.
13) I.R. Bolkland and H.S. Sherif, Nucl. Phys. A694 (2001), 337.
14) W. Peters, H. Lenske and U. Mosel, Nucl. Phys. A642 (1998), 506.
15) B.D. Serot and J.D. Walecka, "The relativistic Nuclear Many Body Problem", J. W. Negele and E. Vogt, editors, *Adv.Nucl.Phys.***Vol.16**, page 1, Plenum Press, 1986, and reference therein.
16) R.L. Walker, Phys. Rev. 182 (1969), 1729 .
17) B. Krusche, et al., Phys. Rev. Lett.74 (1995), 3736.

18) W.-T. Chiang et al., Nucl. Phys. A700 (2002), 429.
19) T. Maruyama, H. Fujii, T. Muto and T. Tatsumi, Phys. Lett. B. 337 (1994), 19;
H. Fujii, T. Maruyama, T. Muto and T. Tatsumi, Nucl. Phys. A597 (1996), 645.
20) J. Boguta and S. Bohrmann, Phys. Lett. B102 (1981), 93.
21) S. Hama, B. C. Clark, E. D. Cooper, H. S. Sherif and R. L. Mercer, Phys. Rev. C41 (1990), 2737.
22) W. Botermans and R. Malfliet, Phys. Rep. 198 (1990), 115;
R. Brockmann and R. Machleidt, Phys. Rev. C42 (1990), 1965.
23) C.M.Ko et al., Phys. Rev. Lett.59 (1987), 1084;
Q. Li et al., Phys. Rev. C39 (1989), 849;
B. Blättel, V. Koch and U. Mosel, Rep. Prog. Phys. 56 (1993), 1.
24) T. Maruyama, W. Cassing, U. Mosel, S. Teis and K. Weber, Nucl. Phys. A573 (1994), 653.
25) N.V. Schevchenko, et al., nucl-th/0108031.
26) C. DeTar and T. Kunihiro, Phys. Rev. D39 (1989), 2805;
D. Jido, et al., Nucl. Phys. A671 (2000), 471.
27) D. Jido, et al., Phys. Rev. C66 (2002), 045202.

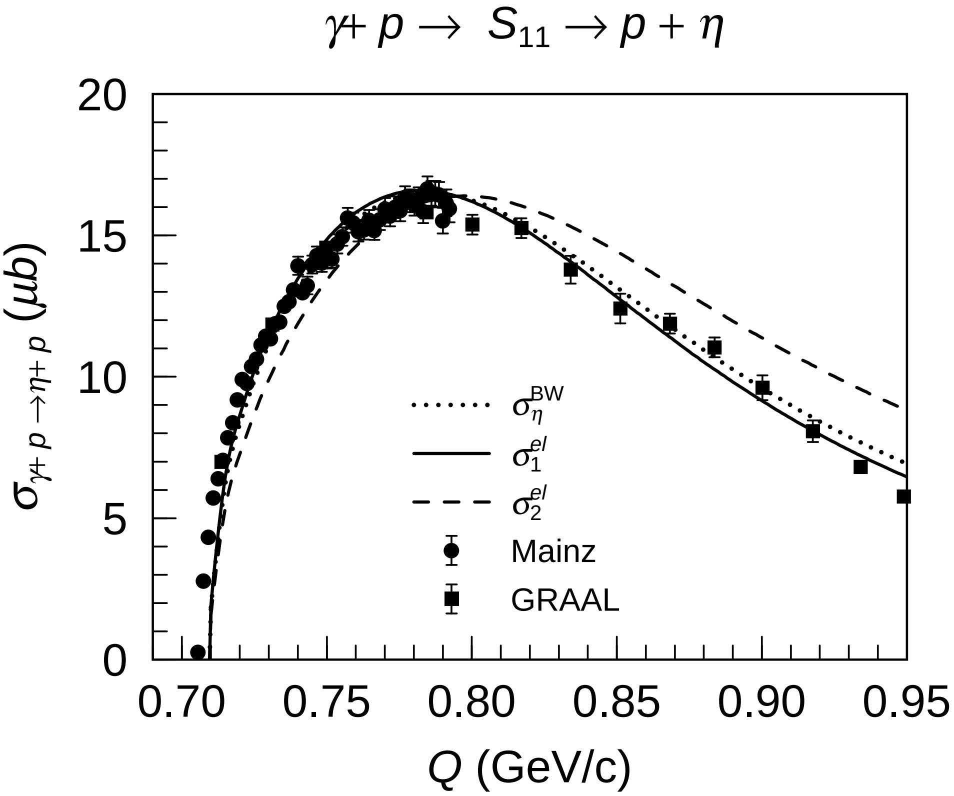

Fig.1 Cross section for eta photo-production with proton targets. The filled circles and squares represent the experimental data of Ref. 17) and 12), respectively. The solid, dashed and dotted curves represent the results of our calculation based on σ_1^{el} and σ_2^{el} and of the phenomenological parametrization σ_η^{BW}, respectively.

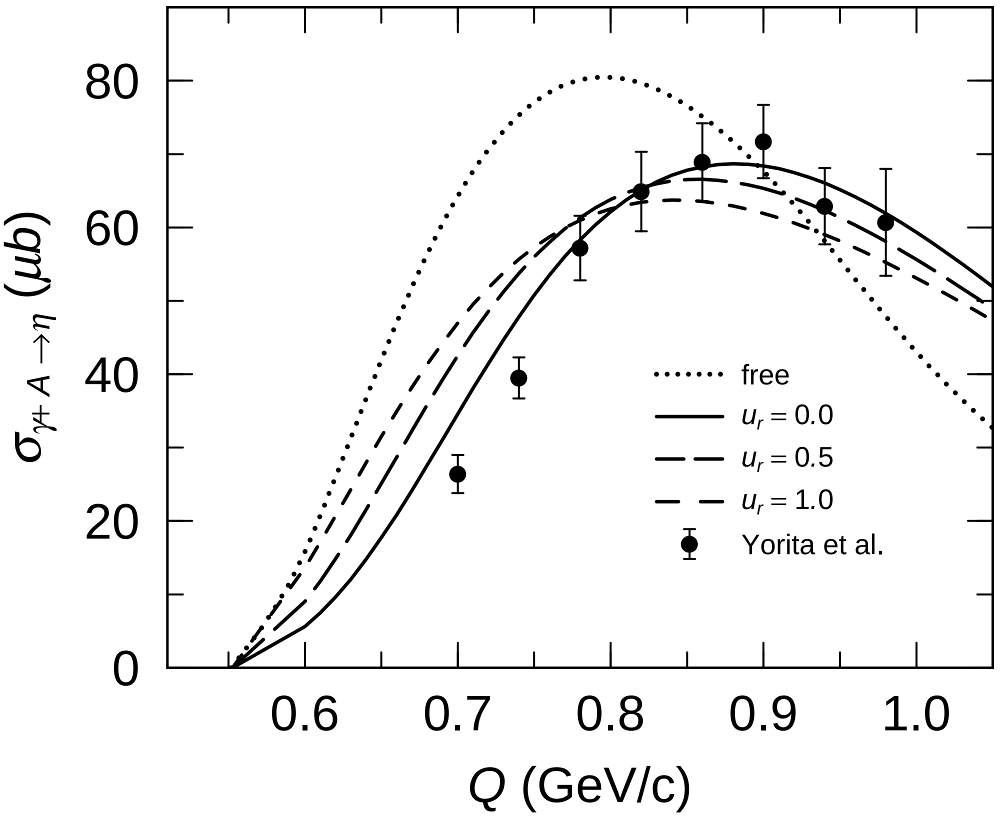

Fig.2 Cross section for eta photo-production with ^{12}C targets. The solid, long-dashed and dashed curves represent the results with $u_r = 0.0, 0.5$ and 1.0, respectively. The nucleon effective mass is taken to be M_N^*/M_N =0.7. The dotted curve represents the results obtained with a free Fermi gas. The filled circles show the experimental data.[9)]

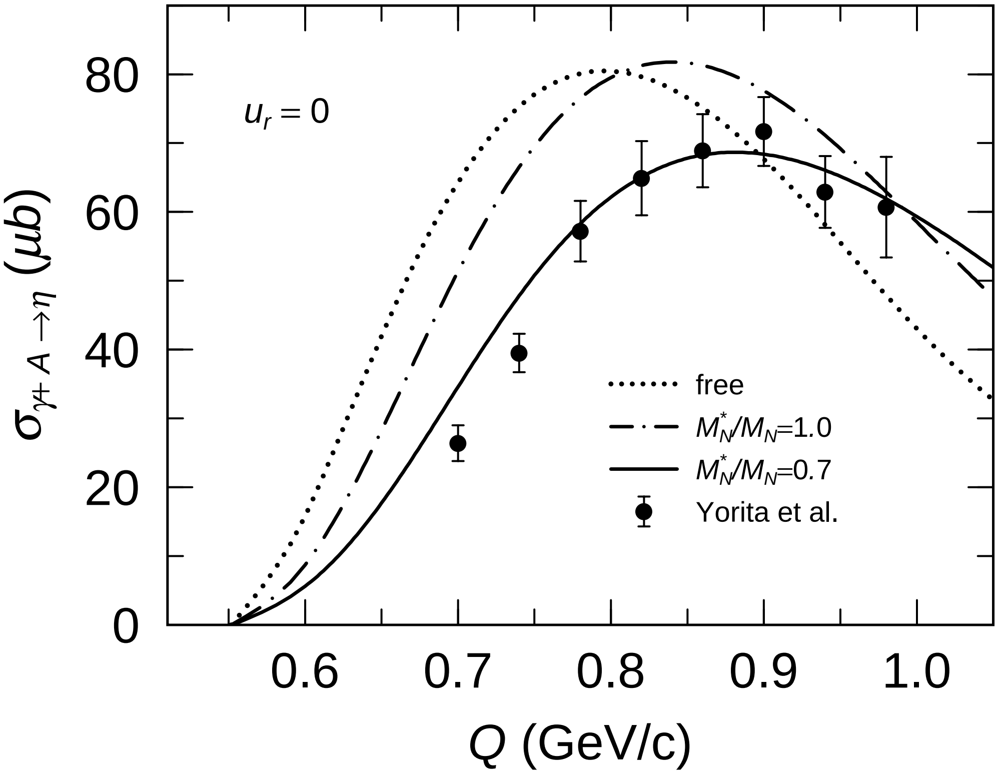

Fig. 3 Cross section for eta photo-production with ^{12}C targets. The solid and dash-dotted curves represent the results obtained with nucleon effective masses M_N^*/M_N =0.7 and 1.0, respectively. The dotted curve represents the results with a free Fermi gas. No mean fields for S_{11} resonances were considered, i.e., $u_r = 0$. The filled circles show the experimental data.$^{9)}$

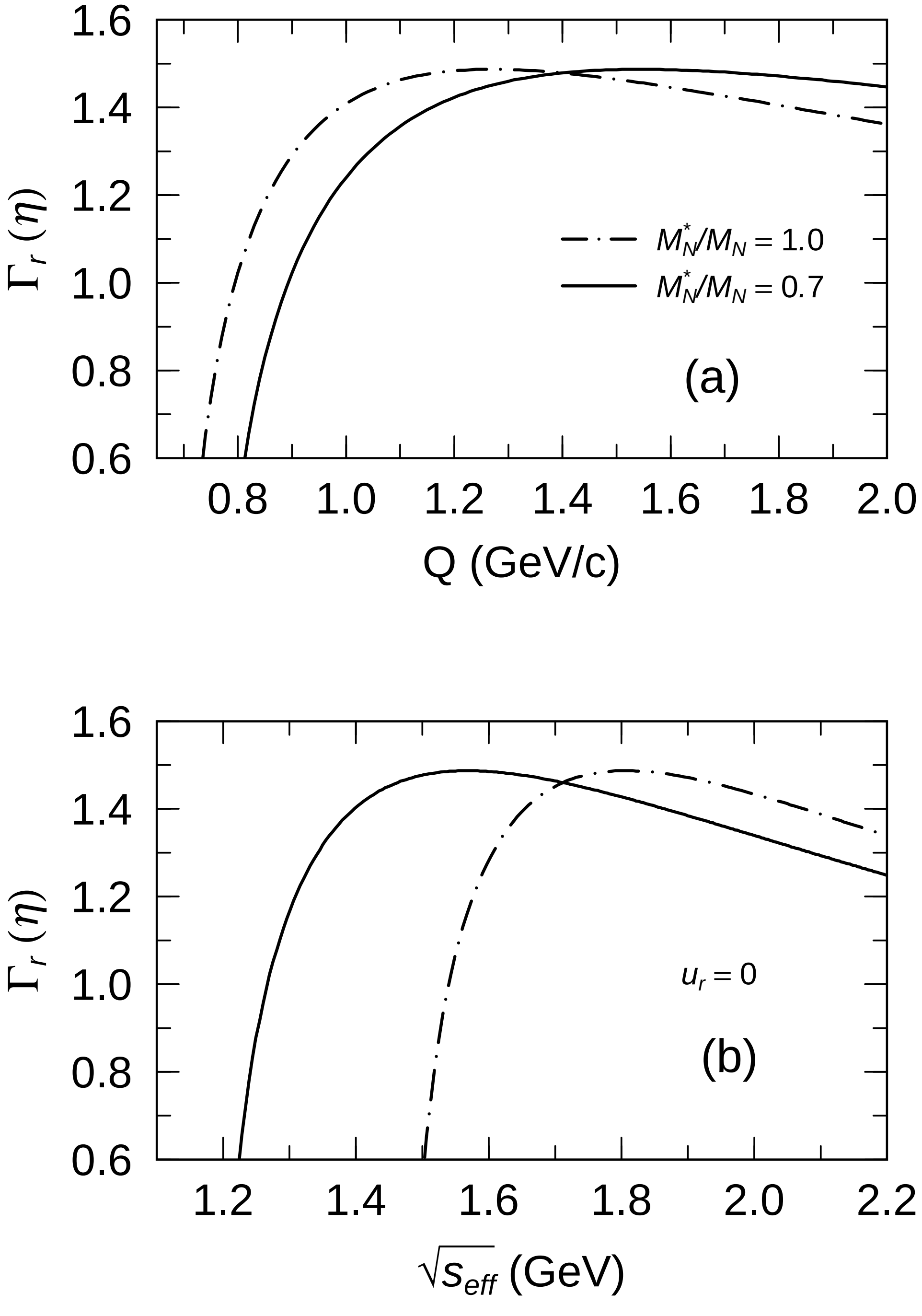

Fig.4 The momentum dependence of the resonance width for $u_r = 0$ is plotted as a function (a) of the photon momentum and (b) of the effective invariant mass (b). The solid and dash-dotted curves represent the results with $M_N^*/M_N = 0.7$ and $= 1.0$, respectively. The details are explained in the text.

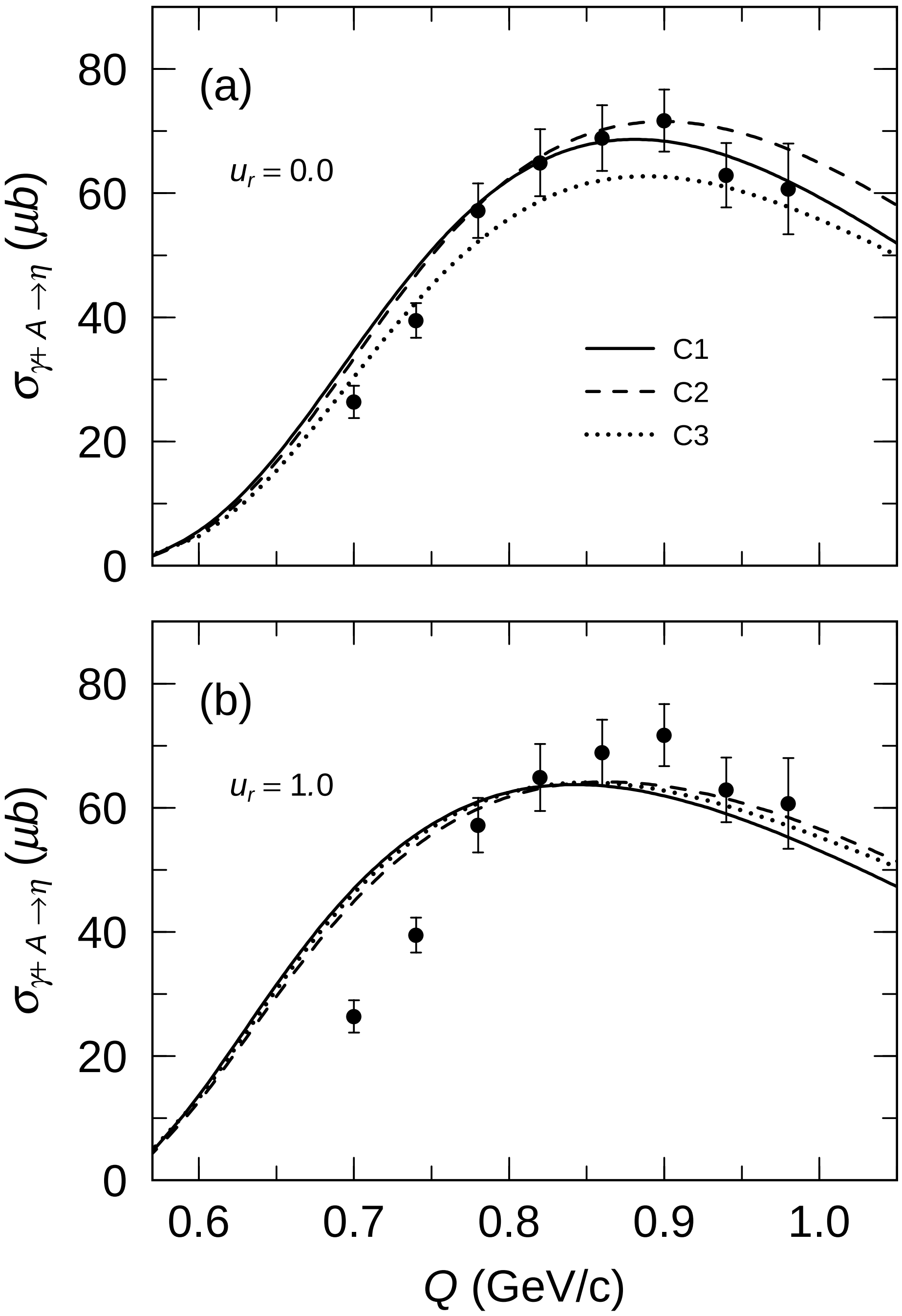

Fig. 5: Cross section for eta photo-production with ^{12}C targets using $M_N^*/M_N = 0.7$, with (a) $u_r = 0$ and (b) $u_r = 1$. The solid, dashed and dotted curves represent the sets of results C1, C2 and C3, whose meanings are explained in the text. The filled circles show the experimental data.[9)]